NJC

Accepted Manuscript

This is an *Accepted Manuscript*, which has been through the Royal Society of Chemistry peer review process and has been accepted for publication.

Accepted Manuscripts are published online shortly after acceptance, before technical editing, formatting and proof reading. Using this free service, authors can make their results available to the community, in citable form, before we publish the edited article. We will replace this *Accepted Manuscript* with the edited and formatted *Advance Article* as soon as it is available.

You can find more information about *Accepted Manuscripts* in the Information for Authors.

Please note that technical editing may introduce minor changes to the text and/or graphics, which may alter content. The journal's standard Terms & Conditions and the Ethical guidelines still apply. In no event shall the Royal Society of Chemistry be held responsible for any errors or omissions in this *Accepted Manuscript* or any consequences arising from the use of any information it contains.

ROYAL SOCIETY OF CHEMISTRY

www.rsc.org/njc

Dehydration of $AlPO_4$-34 studied by variable-temperature NMR, XRD and first-principles calculations

Jure Varlec,[a] Andraž Krajnc,[a,b] Matjaž Mazaj,[a] Alenka Ristić,[a] Kalju Vanatalu,[c] Andres Oss,[c] Ago Samoson,[c] Venčeslav Kaučič[a] and Gregor Mali*[a]

[a]National Institute of Chemistry, Hajdrihova 19, SI-1001 Ljubljana, Slovenia.
[b]Jozef Stefan International Postgraduate School, Jamova cesta 39, SI-1000 Ljubljana, Slovenia.
[c]Technomedicum, Tallinn University of Technology, Akadeemia 15A, Tallinn, Estonia.

Corresponding author: G. Mali (gregor.mali@ki.si)

Abstract

Microporous zeolite-like aluminophosphate $AlPO_4$-34 is a very promising material for water-adsorption-based thermal energy storage. To obtain better understanding of the dehydration of this material, a detailed variable-temperature nuclear magnetic resonance (NMR), X-ray diffraction (XRD), and first-principles calculation study was carried out. Unlike the previous studies, this one detected three distinct phase transitions during the dehydration. The fully hydrated phase of $AlPO_4$-34 first loses one water molecule per unit cell and transforms to the partly dehydrated phase I (space group P1). The molecule that was expelled first is the molecule that was initially located within the double six-membered ring and was very weakly coordinated to aluminium atom and not involved in hydrogen bonds. During the second phase transition a water molecule is expelled from each chabazite cage. The obtained partly dehydrated phase II (space group P-1) contains six water molecules in each chabazite cage and four water molecules coordinated to octahedral aluminium. The third transition leads to the completely dehydrated material. Structures of both partly dehydrated phases of $AlPO_4$-34 were determined by the Rietveld method. Variable-temperature NMR and XRD detected very different phase-transition temperatures. This was due to very different sample packing, which significantly influenced the rate of water removal. The confirmation that the two techniques observed the same phases of $AlPO_4$-34 was obtained by the first principles calculations of NMR observables. Using the XRD-based structural models, the calculations predicted ^{31}P and ^{27}Al isotropic chemical shifts that agreed well with the observed ones.

Introduction

Zeolite-like microporous aluminophosphates have been known for more than three decades. They were developed as an extension to the well-known aluminosilicate zeolites and were at first considered as candidates for catalysts. Lately, interest in these materials has increased because of their very promising properties for gas separation and storage and for water-adsorption-based thermal energy storage or energy allocation.[1–5] One of the most promising microporous aluminophosphates for energy-storage applications and applications in adsorption-based heat pumps and chillers is $AlPO_4$-34,[6,7] which exhibits chabazite topology. In the temperature range between 40 °C and 140 °C it can store 240 kWh of energy per m^3, it adsorbs water in a very narrow relative-pressure range, and it is hydrothermally stable and thus enables reversible adsorption and desorption without a significant decrease of the storage capacity.[5] In Figure 1, water-loading capacities of four different materials are compared: silica gel is a widely utilized water adsorbent, which is, however, characterized by a rather weak hydrophilicity; water-loading capacity is much higher in silico-aluminophosphate SAPO-34,[1] a commercially recognized adsorbent for chillers; even higher capacity was recently demonstrated for aluminium-based metal-organic framework material MIL-160,[8] which combines highly hydrophilic character and large pore volume; maximal water-loading capacity of $AlPO_4$-34 is approximately equal to the capacity of MIL-160, but its regeneration at the temperature of 95 °C is much more efficient.[5]

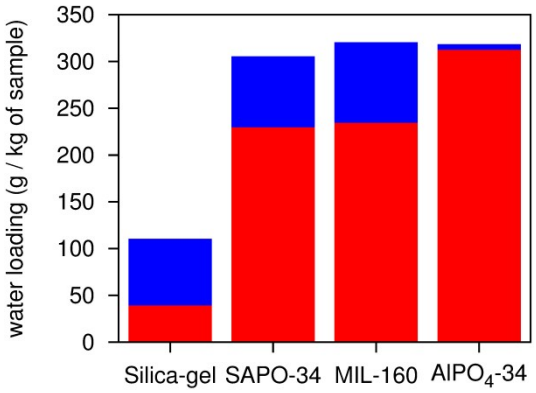

Figure 1. Comparison of water-loading capacities for four different materials at two different desorption temperatures (95 °C – red bars, 140 °C – blue bars). The data presented in the graph were obtained from the literature.[1,5,8]

The great application potential of the above described adsorbents implies the necessity for a better understanding of water sorption mechanism, which might enable one to design more efficient new adsorbents or find better ones among the already known materials. In $AlPO_4$-34 water sorption was already studied to some extent. In 2000, Tuel et al.[6] solved the structure of

the hydrated phase of the aluminophosphate and determined that each unit cell of $AlPO_4$-34 at the temperature of 20 °C comprises 12 water molecules; four of these molecules were coordinated to two hexa-coordinated aluminium sites, one was coordinated to a penta-coordinated aluminium atom, and one was considered as a fifth neighbour of a '4+1' coordinated aluminium atom (Figure 2). The remaining six water molecules were located inside the micropores and were forming strongly hydrogen-bonded network. Variable-temperature XRD measurements performed by the same researchers showed that at about 25 °C the hydrated phase undergoes a phase transition. It was proposed that the high-temperature phase was partly dehydrated and that it contained 11 water molecules per unit cell. This phase of $AlPO_4$-34 could not be isolated experimentally and its structure could not be solved. A subsequent computational study,[9] however, suggested that the water molecule that would be first expelled from the material might be the so-called quasi-framework water molecule, i.e. the molecule that in the fully hydrated phase gives rise to the 4+1 coordinated aluminium atom and is located inside the double six-ring. For a coordinated molecule this water molecule is unusually distant from the aluminium atom and it is also not involved in the hydrogen-bonded network. Expelling this molecule from $AlPO_4$-34 should not modify the framework and the positions of the remaining water molecules significantly. The partly dehydrated phase was found to transform into a completely dehydrated, highly-symmetric rhombohedral form at about 50 °C.[6]

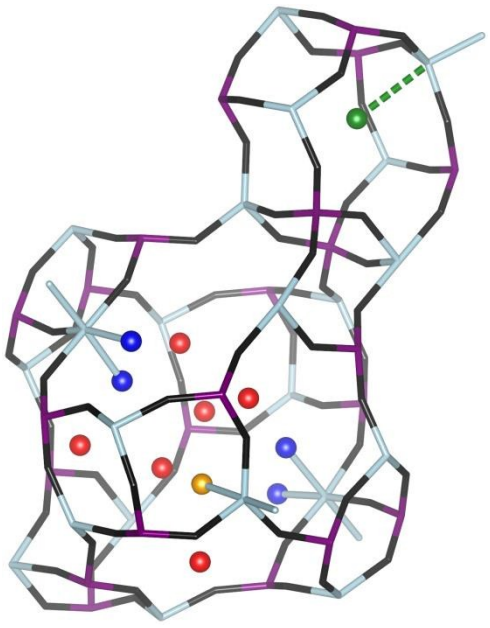

Figure 2. The chabazite cage and the double six-membered ring of the fully hydrated $AlPO_4$-34. Framework is represented with sticks and water oxygen atoms are represented by spheres. (purple: phosphorous; light blue: aluminium; black: framework oxygen; blue: water oxygen atoms attached to six-coordinated aluminium; yellow: water oxygen atom attached to five-coordinated aluminium; green: water oxygen atom proximal to the 4+1 coordinated aluminium;

red: water oxygen atoms not coordinated to the framework) Hydrogen atoms of the water molecules are omitted for clarity. Image generated with VESTA.[10]

In the above described study very useful structural constraints were obtained by magic-angle spinning NMR measurements.[6] Actually, solid-state NMR spectroscopy very often provides valuable insight into materials, which is complementary to the one obtained by diffraction techniques. That is why, in an attempt to improve our understanding of water desorption from $AlPO_4$-34, we conducted a detailed in-situ NMR study, complemented by XRD measurements and first-principles calculations.

Experimental and computational

Synthesis. $AlPO_4$-34 was hydrothermally synthesized from a fluoride medium using piperidine as a structure-directing agent. The molar ratio of reactants in the reaction gel was Al_2O_3 : P_2O_5 : HF : 100 H_2O : 2 piperidine. Crystallization was performed in Teflon-lined stainless steel autoclaves at 200 °C for two days. The as-synthesized sample was thermally treated in an air flow at 650 °C over night. The calcined sample was exposed to saturated solution of ammonium chloride in water for 7 days at room temperature in order to prepare fully hydrated sample.

NMR spectroscopy. Solid-state NMR experiments were carried out on a narrow-bore 600 MHz Varian NMR spectrometer using a 4.0 mm custom-made laser-heated variable-temperature HX MAS probe. Larmor frequencies for ^{31}P, ^{27}Al, and ^{1}H nuclei were 242.70, 156.22, and 599.54 MHz respectively. Sample spinning frequency was 8 kHz in all experiments. Temperature inside the rotor was controlled indirectly by the appropriate power of the lasers. Prior to the measurements, the laser power and the temperature scale were calibrated using $Pb(NO_3)_2$ as a calibration standard.[11] Spectra were measured at different temperatures ranging between 40 °C and 280 °C. ^{31}P MAS spectra were taken with a single scan, using a $\pi/2$ excitation pulse with the duration of 3.35 μs. ^{27}Al MAS spectra were recorded using a $\pi/9$ excitation pulse of 1 μs and 128 repetitions. The recycle delay was set to 0.5 s. ^{1}H MAS spectra were collected using a single-pulse experiment with 8 repetitions and recycle delay of 5 s. The $\pi/2$ pulse duration was 3.8 μs. Dynamics of water molecules were probed by measuring series of ^{1}H Hahn echos at different temperatures. $\pi/2$ and π pulses of 3.8 and 7.6 μs, respectively, and rotor-synchronized interpulse delays ranging from 125 μs to 20 ms were used. Each echo was obtained with four repetitions and recycle delay was 3 s. The selected experimental protocol measures the effective transverse relaxation time T_2*, which differs from the true transverse relaxation time T_2 when molecular or spin diffusion takes place in the sample and when internal or background

magnetic-field gradients are present.[12,13] Because, for our study, T_2* offered adequate qualitative insight into the variation of the dynamics of water molecules with temperature, no extraction of the true T_2 was attempted.

X-ray diffraction and crystallography. Variable-temperature powder X-ray diffraction patterns were recorded on a PANalytical X'Pert PRO high-resolution diffractometer with CuKα1 radiation (λ = 1.5406 Å) in the 2θ range from 8.5° to 90° using a step of 0.013°. Diffraction patterns were recorded in steps of 5 °C from 25 °C to 40 °C and in steps of 2 °C from 40 °C to 80 °C in air. The detailed temperature-programmed regime enabled the detection of two isolated phases, which previously have not been detected (partly dehydrated phases I and II). The patterns recorded at 50 °C and 56 °C were used for the Rietveld refinement of phase I and phase II, respectively.

Rietveld refinement procedure was carried out using the Topas-Academic v.4 software package.[14] Background and profile of the XRD patterns were first refined in Le Bail fit,[15] before the inclusion of any structure parameters. The structural model of the fully hydrated $AlPO_4$-34, determined by Tuel et al.,[6] was used as the initial structural model for the crystal structure refinement of the partly dehydrated phase I. Whole Rietveld analysis of the structure included gradual refinement of the unit cell parameters, temperature factors and atomic positions. Restraints on all Al-O and P-O distances as well as AlO_4 and PO_4 tetrahedra were employed. Exclusion of one water oxygen atom from the initial model significantly improved the fit. At the final stage, Rietveld refinement of the dehydrated phase I involved 163 independent parameters. The obtained structural model of phase I was subsequently used as a starting model for the structure determination of the partly dehydrated phase II. The same Rietveld analysis procedure was used as in the case of phase I. Exclusion of an additional oxygen atom located in the chabazite cage and the inclusion of the centre of inversion (increasing symmetry from *P1* to *P-1*) improved the fit and led to acceptable final figures of merit (Rp = 0.097, Rwp = 0.108). Rietveld plots, detailed refinement parameters and fractional atomic coordinates are available in the Supplementary data.

Computational. First principles calculations were performed using the Density Functional Theory (DFT) approach as implemented in the Quantum ESPRESSO[16] plane-wave pseudopotential code (version 5.1.2). The PBEsol[17] functional (which is of the Generalized Gradient Approximation type) was used with Projector Augmented Wave pseudopotentials from PSLibrary[18] (version 0.3.1). NMR chemical shifts and quadrupolar coupling constants were calculated using the Gauge-including Projector Augmented Wave[19] approach implemented in the QE-GIPAW[20] module of Quantum ESPRESSO. Calculations were performed with 80 Ry and 560

Ry kinetic energy cutoffs for wavefunctions and charge density, respectively. A 3×3×3 Monkhorst-Pack[21] k-point grid was employed to ensure that stress and forces were sufficiently converged for geometry optimization. The latter was done using the BFGS algorithm with convergence thresholds of 10^{-3} a.u., 10^{-2} a.u. and 2 kbar for energy, forces and pressure, respectively; it turned out that the pressure threshold was the strictest, ensuring that energy and forces were much better converged than specified, by about two orders of magnitude on average. It must be noted that it was not possible to obtain better pressure convergence neither with higher cutoffs nor with different pseudopotentials. The achieved convergence, however, is deemed sufficient and is about the same as that achieved for the hydrated $AlPO_4$-34 before, with the caveat that, unlike Poulet et al.,[9] we have found gamma point calculations insufficient. QE-GIPAW module yielded chemical shielding parameters and quadrupolar parameters ($C_Q = eQV_{zz}/h$, η_Q). The calculated ^{31}P and ^{27}Al isotropic chemical shifts (δ_{calc}^{iso}) were obtained from the corresponding isotropic shielding parameters (σ_{calc}^{iso}) using the relation $\delta_{calc}^{iso} = \sigma_{ref}^{iso} - \sigma_{calc}^{iso}$. The reference isotropic shielding parameter (σ_{ref}^{iso}) was determined by the linear regression fit so that the agreement between the calculated and the measured isotropic chemical shifts was the best. For ^{31}P σ_{ref}^{iso} was 279.4 ppm and for ^{27}Al σ_{ref}^{iso} was 571.3 ppm.

Results and discussion

The microporous aluminophosphate $AlPO_4$-34, exhibiting chabazite topology, was synthesized, calcined and hydrated as described in the Experimental section. Then the material was subjected to the detailed solid-state NMR analysis. Variable-temperature ^{31}P MAS NMR spectroscopy quite unexpectedly detects three phase transitions during the dehydration of the material (Figure 3). The spectrum of the fully hydrated phase exhibits five signals belonging to six crystallographically inequivalent P sites (two crystallographic sites give rise to a single strong signal with twice the intensity of the other individual signals; see Figure 3 and Supplementary Information). The first transition occurs at about 70 °C, but does not lead to a significant change of the spectrum. The spectrum is still composed of six contributions, which, however, overlap more extensively than the contributions in the spectrum of the initial phase. At 100 °C the ^{31}P MAS NMR spectrum of $AlPO_4$-34 simplifies substantially and exhibits only three well resolved signals. With the increasing temperature the isotropic chemical shifts of these three signals slightly vary, but the overall appearance of the spectrum is not altered significantly. At about 180 °C the ^{31}P signal at -29 ppm starts to prevail and finally remains the only signal in the spectrum of the completely dehydrated material.

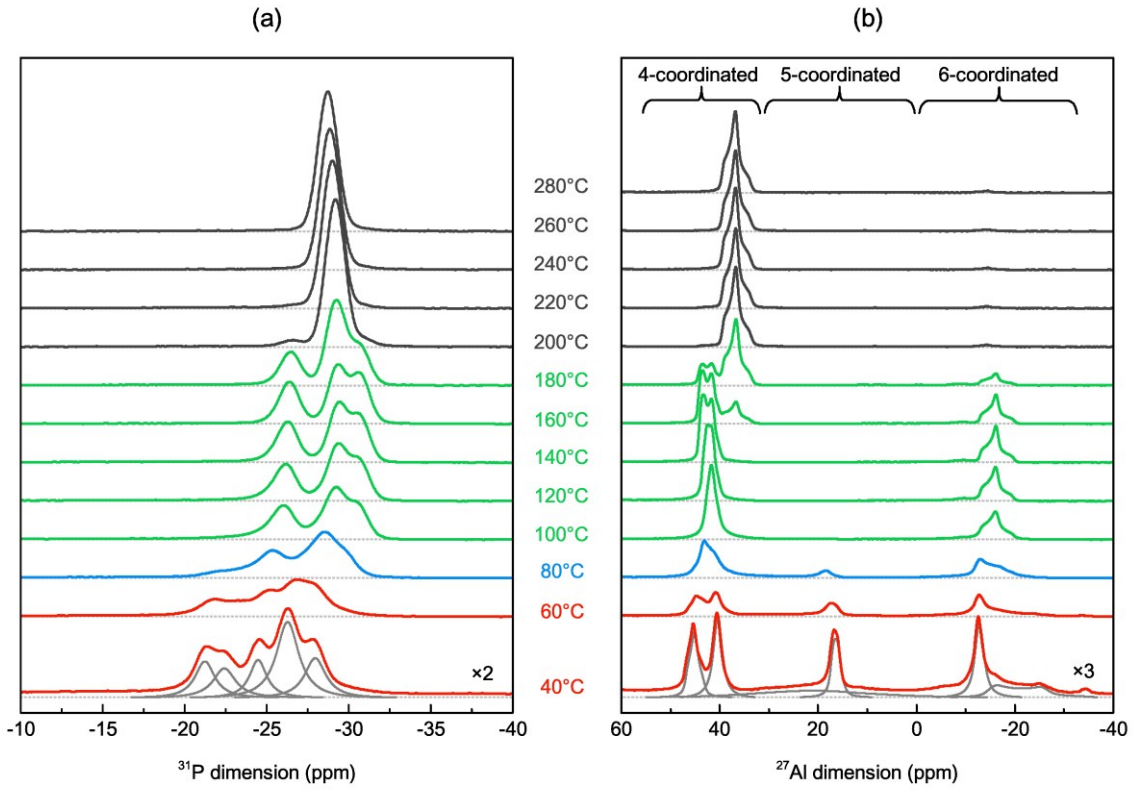

Figure 3. ^{31}P (a) and ^{27}Al (b) MAS NMR spectra of $AlPO_4$-34 recorded at different temperatures. The spectra that were assigned to different phases of the aluminophosphate are plotted with different colours. ^{27}Al spectra show only signals that belong to central transitions. Decomposition of the ^{31}P and ^{27}Al NMR spectra recorded at 40 °C is shown at the bottom.

^{27}Al MAS NMR spectra, too, suggest the existence of three phase transitions (Figure 3), although the detected changes in these spectra appear to be more continuous than the changes in the ^{31}P MAS NMR spectra. This might be due to the fact that the appearance of the Al spectrum is determined not only by the isotropic chemical shifts but also by the electric quadrupolar coupling parameters; the quadrupolar coupling constants can change substantially if the neighbours of Al atoms change (for example due to the removal of water molecules) or even if the dynamics of the neighbours change (due to the change of the dynamics of water molecules at increased temperature). The spectrum of the fully hydrated phase exhibits five signals with well-defined quadrupolar lineshapes and a broad contribution in the chemical shift range between 40 and 5 ppm (see also Supplementary Information). All six signals have approximately equal intensities. The five well defined signals belong to two four-coordinated (47 and 41 ppm), one five-coordinated (18 ppm), and two six-coordinated Al sites (both resonating at -12 ppm). The broad contribution could be assigned to the 4+1 coordinated Al site. Because the quasi-framework water forms a very weak coordination bond with this Al site and is not involved in hydrogen bonds, its position is the least defined. It is known from the previous ab-initio

molecular dynamics study[9] that this molecule is subjected to a strongly anharmonic potential inside the double six-ring and exhibits a large amplitude of oscillation around the average, which leads to the smearing of the corresponding Al signal. At about 70 °C the lineshapes and chemical shifts in the ^{27}Al MAS NMR spectrum start changing, but the number of signals remains the same. At 100 °C the spectrum of $AlPO_4$-34 changes significantly – the signal of the five-coordinated Al vanishes and only the signal of the four-coordinated and the signal of the six-coordinated Al remain. The former signal at 44 ppm is twice as strong as the latter signal at -11 ppm. Obviously, as the ^{31}P spectrum, the ^{27}Al spectrum at 100 °C also reflects the increased symmetry of $AlPO_4$-34 and suggests that the obtained phase comprises only three inequivalent Al sites, two four-coordinated and one six-coordinated. It is interesting to observe that further heating of the sample leads to continuous changes in the shape of the NMR signal of the four-coordinated Al but not in the shape of the six-coordinated Al. This might be a consequence of the increased mobility of water molecules within the micropores, which perhaps induces slight changes also in the framework itself (it should be noted that the framework of $AlPO_4$-34 is quite flexible and that its symmetry and the size of the unit cell change substantially during the dehydration). At 180 °C a new NMR signal of four-coordinated Al starts rising at 39 ppm. The signals at 44 and -11 ppm start decreasing and vanish completely at about 220 °C.

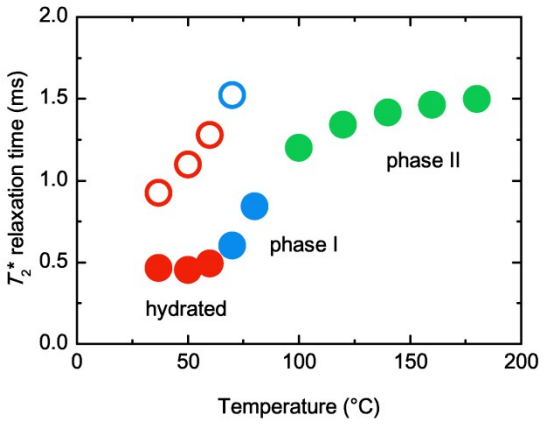

Figure 4. Variation of ^{1}H effective transverse relaxation time with temperature for water molecules adsorbed within $AlPO_4$-34. At low temperatures the relaxation curve can be described as a bi-exponential curve (open circles: weak, slowly relaxing contribution; filled circles: strong, quickly relaxing contribution). At about 100 °C the weak contribution vanishes and the relaxation curve becomes mono-exponential. Colours of the symbols in the plot indicate the tentative assignment to individual phases of the aluminophosphate. The assignment is based on the phase transitions detected in the ^{31}P and ^{27}Al MAS NMR spectra.

Resolution of ^{1}H MAS NMR spectra is not sufficiently high to enable one to resolve the contributions of the framework and non-framework water molecules. Interesting information can, however, be obtained from the transverse relaxation measurements (Figure 4). Up to about 100 °C the ^{1}H transverse relaxation curve can be described as a bi-exponential curve, composed of a low-intensity, slowly relaxing contribution (weak contribution) and a high-intensity, quickly relaxing contribution (strong contribution). At 100 °C the weak contribution vanishes and the relaxation curve becomes mono-exponential. The weak contribution might be ascribed to relatively mobile water molecules, which are neither closely coordinated to the framework nor involved in the strong hydrogen-bonded network. Fast motion namely averages out proton-proton dipolar couplings and reduces their effect on the transverse relaxation time. The best candidates for the mobile water molecules are the ones that give rise to the 4+1 and perhaps even to 5 coordinated Al sites, i.e. to two Al sites whose signals vanish from the ^{27}Al MAS NMR spectrum up to the temperature of 100 °C. Of course, with the increasing temperature the transverse relaxation of the protons of the remaining adsorbed water molecules also becomes slower and slower. This is not surprising, because even the coordinated and hydrogen-bonded water molecules within the chabazite cage become more and more mobile.

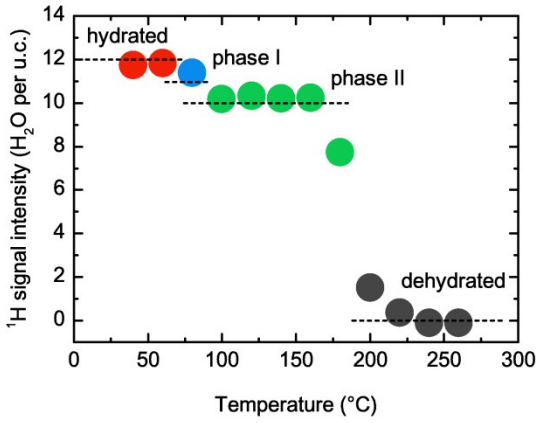

Figure 5. Integral of the ^{1}H MAS NMR signal of $AlPO_4$-34 as a function of temperature. Maximal intensity is normalized to 12, i.e. to the expected number of water molecules in one unit cell of the fully hydrated material. Horizontal dashed lines are plotted at the values of 12, 11, 10 and 0. Colours of the symbols in the plot again indicate the tentative assignment to individual phases of the aluminophosphate.

Quantitative analysis of the ^{1}H MAS NMR spectra is not easy. This is partly because of the presence of non-negligible background signals and partly because the intensities of the spinning sidebands of the water contribution change continuously with the increasing temperature. Careful integration of the water signal and subtraction of the background signals, however,

provide very interesting insight into the dehydration of $AlPO_4$-34. During heating the total integral of the ^1H MAS NMR spectrum shows three distinct steps (Figure 5). In the first one at about 70 °C the integral drops for approximately 1/12, which corresponds to the loss of approximately one water molecule per unit cell. The next step is at about 100 °C and corresponds to the loss of another water molecule. In the last step between about 160 °C and 220 °C the integral drops to zero. This drop corresponds to the loss of ten water molecules. The variation of the ^1H NMR integral with temperature agrees very well with the observed changes in the ^{31}P and ^{27}Al MAS NMR spectra. It indicates that the first three phases of $AlPO_4$-34, the fully hydrated one and the two that are obtained by heating to about 70 °C (phase I) and to about 100 °C (phase II), contain rather similar amount of water. It also shows that up to the temperature of 160 °C non-framework water, which represents a half of all the water, is not expelled from the chabazite cages of $AlPO_4$-34. In fact, the decrease in the total intensity of the ^1H MAS NMR signal above 160 °C is well correlated with the increase of the ^{27}Al and ^{31}P signals that belong to the completely dehydrated phase and with the decrease of the ^{27}Al signal of the six-coordinated Al. This suggests that framework water molecules at the six-coordinated Al sites and the non-framework water molecules are expelled from $AlPO_4$-34 practically simultaneously. It seems that either detachment of the framework water molecules from the Al sites or the perturbation of the clusters of non-framework water molecules destabilizes the hydrogen-bonded network and leads to a rather abrupt removal of water from the material. The NMR experiments cannot tell what happens first, the detachment of the coordinated water molecules or the extraction of the non-framework water molecules.

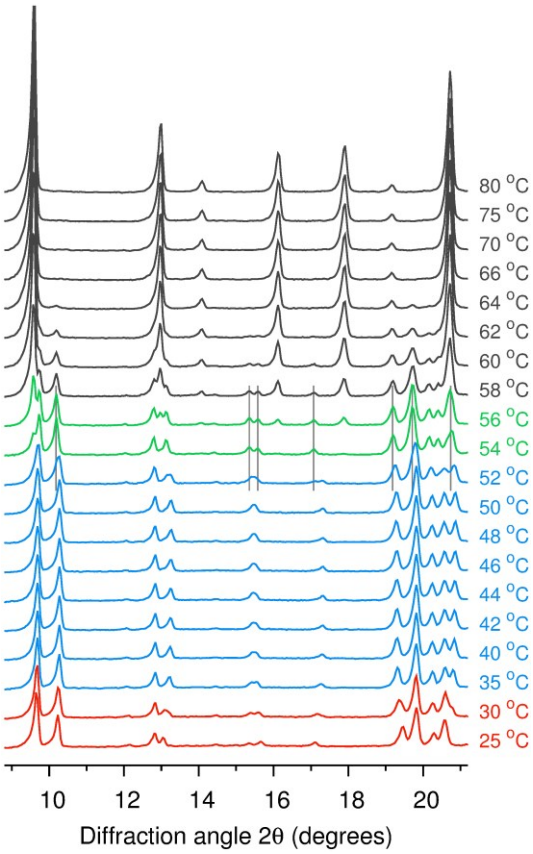

Figure 6. Powder XRD patterns of $AlPO_4$-34 as a function of temperature. Different colours are used for diffraction patterns that, presumably, correspond to the different phases of the aluminophosphate as detected by MAS NMR measurements. Some differences between the diffraction patterns of the phase I (blue) and phase II (green) are marked with thin vertical lines.

The observed changes in the NMR spectra are in disagreement with the results of previous analyses of the dehydration of $AlPO_4$-34, which detected only two phase transitions that occurred at 25 and 50 °C.[6] The different phase-transition temperatures detected by NMR and XRD can be (i) due to the different thermometers employed for the two experiments (external calibration of laser power with $Pb(NO_3)_2$ for NMR versus a built-in thermometer in the XRD apparatus), (ii) due to different rate of heating, and (iii) mostly due to different sample packing in the two experiments (the sample is spread onto a flat sample holder for XRD measurements but densely packed and tightly closed into the rotor for NMR measurements). These differences, however, do not explain why the previous XRD studies detected only two phase transitions. To answer this question, variable-temperature XRD measurements were conducted again. This time, using a smaller temperature step in the XRD analysis, the three phase transitions were detected. The temperatures of these phase-transitions were 35, 54, and 58 °C (Figure 6). According to XRD, the third hydrated phase (presumably corresponding to phase II detected by NMR) can be observed only in a very narrow temperature interval between 54 °C and 56 °C. This

is probably the reason why this phase was not detected in the previous XRD-based studies. It is interesting that this particular phase can be much more easily detected by NMR. Within the NMR rotor the phase sustains a much wider temperature interval most probably because of the different packing of the sample. Also, whereas the differences in the diffraction patterns of phases I and II are tiny, the differences in the NMR spectra between the two phases are significant. This is mostly because of the increased crystal symmetry, which leads to the reduction of the number of the distinguished ^{31}P and ^{27}Al signals.

Four diffraction patterns that belong to four different phases of $AlPO_4$-34 were recorded with higher resolution and analysed more thoroughly. The diffraction patterns at 25 °C and 80 °C correspond to the already known fully hydrated and completely dehydrated phases, respectively. The diffraction patterns recorded at 50 °C and at 56 °C were subjected to the Rietveld analysis. For this analysis the structural model of the fully hydrated phase was used as the initial structural model. Information obtained by NMR spectroscopy was also employed; it was taken into account that the amount of water in phases I and II is not much different from the amount of water in the fully hydrated phase (and most probably equal to 11 and 10 water molecules per unit cell of phase I and phase II, respectively), that phase I has the same crystal symmetry as the fully hydrated phase, and that phase II has higher crystal symmetry which comprises inversion symmetry. The structural models were successfully refined and the structure parameters for the two phases are gathered in Table 1 and in Supplementary material. Rietveld refinement for phase I proposes a structural model with 11 water molecules in the unit cell, seven molecules within the pore and four molecules coordinated to two six-coordinated Al sites. A more detailed comparison of structures of the fully hydrated and the partly dehydrated phase I is shown in Figure 7. In the fully hydrated phase five water molecules are coordinated to Al centres and six water molecules are adsorbed within the pore. Additional water molecule is located slightly off-centre of the small double six-ring cage and gives rise to a 4+1 coordinated Al site. During the transformation to phase I, this water molecule is expelled from the structure. The water molecule that was coordinated to the five-coordinated Al site moves away from this site towards the water cluster located in the centre of the chabazite cage. The remaining water molecules in the cluster undergo a minor positional rearrangement, but their isotropic displacements become significantly larger than in the fully hydrated structure. The observed loss of one water molecule is in agreement with the proposition of the previous computational analysis as well as with the results of NMR experiments.

Table 1: Structure parameters and refinement data for the fully hydrated $AlPO_4$-34 and the partly dehydrated phases I and II. The parameters of the fully hydrated phase were not refined and were added for comparison.[6]

Structure parameters and refinement details	**Fully hydrated**	**Phase I**	**Phase II**
Unit cell parameters			
a (Å)	9.026	9.0197(2)	9.0832(3)
b (Å)	9.338	9.2738(2)	9.2516(2)
c (Å)	9.508	9.5995(2)	9.6682(3)
α (°)	95.1	95.217(2)	95.098(3)
β (°)	104.1	104.901(2)	104.216(2)
γ (°)	96.6	95.270(3)	95.889(3)
V (Å^3)	766.38	767.20(4)	777.92(4)
space group	*P1*	*P1*	*P-1*
Z	1	1	2
T (°C)	25 °C	50 °C	56 °C
R_p, R_{wp}, R_{exp}		0.072, 0.081, 0.009	0.097, 0.108, 0.01

For phase II the structural model proposed by Rietveld refinement contains ten water molecules in the unit cell, six water molecules are within the pore and four molecules remain coordinated to two six-coordinated Al sites (Figure 7). In agreement with ^{27}Al MAS NMR, there are no five-coordinated Al sites in the material and the structural model has an inversion centre in the middle of the chabazite cage. As expected, isotropic displacements of the water molecules within the chabazite cage become even larger than in phase I. This is in agreement with the observed prolongation of the ^{1}H transverse relaxation time. Water molecule expelled from the structure is the one that was initially coordinated to the five-coordinated Al site.

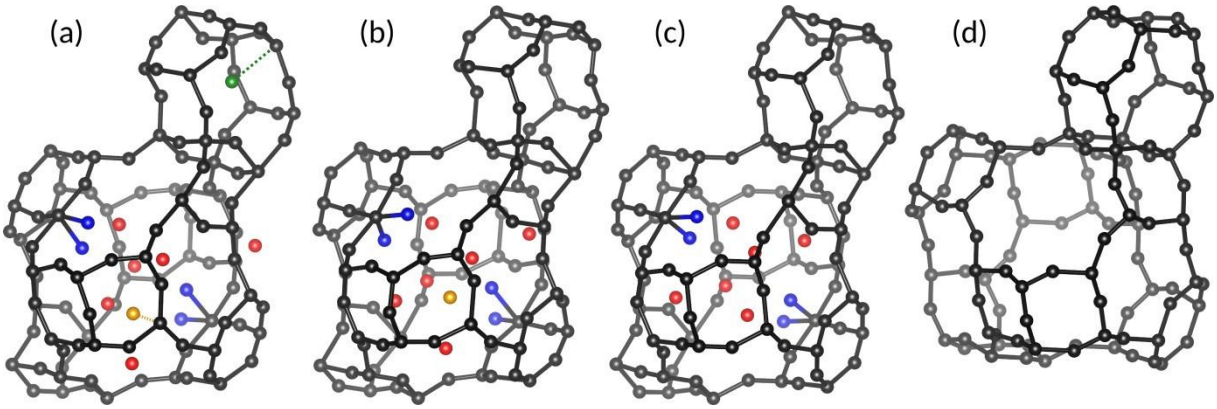

Figure 7. The chabazite cage and the double six-membered ring in different phases of $AlPO_4$-34: (a) fully hydrated; (b) phase I; (c) phase II; (d) dehydrated. Black: framework atoms (Al, P and O); blue: water oxygen atoms coordinated to framework Al; red: water oxygen atoms not coordinated to the framework; green and yellow: water oxygen atoms that are expelled during the transitions to phase I and II, respectively.

Because of the very different phase-transition temperatures detected by NMR and XRD, we decided to verify if the two experimental techniques actually observe identical phases of $AlPO_4$-34. We decided to employ the structural models obtained from the XRD analysis and, using first-principles calculations, predict NMR observables. Comparison between the measured and predicted values of ^{31}P and ^{27}Al isotropic chemical shifts and ^{27}Al quadrupolar coupling constants could answer the above question. Before starting the calculation of NMR observables, we inserted hydrogen atoms into the XRD structural models of the fully hydrated phase and of the two partly dehydrated phases. Water molecules thus formed were oriented randomly. Between 10 and 20 random structures were generated per phase. All the models were subjected to the DFT-based geometry optimization of both atomic positions and unit cell shape. For phase II, P-1 symmetry was enforced. Depending on the initial positions of hydrogen atoms, optimization led to slightly different relaxed models. The ground-state energies of the lowest-energy structural models of the fully hydrated and partly dehydrated phases were compared to the energy of the completely dehydrated phase of $AlPO_4$-34 and to the energy of the proper number of isolated water molecules (Figure 8). The comparison shows that the energies of all three hydrated phases are lower than the sum of the energies of the empty $AlPO_4$-34 and of the water molecules. In other words, first principle calculations confirm that all three hydrated phases are at least partially stable, being local energy minima with negative binding energies. They also show that the fully hydrated phase is the lowest-energy, most-stable phase of $AlPO_4$-34. Thus, in spite of known deficiencies of fully local correlation functionals (of which PBEsol is an example) regarding description of dispersive interactions, known to be important when

studying structural properties of water,[22] the obtained sensible binding energies provide some support to the reliability of the calculations.

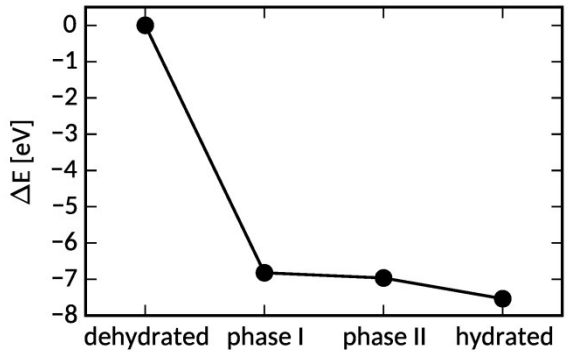

Figure 8. Energy differences between phases of $AlPO_4$-34, per unit cell, referenced to the dehydrated phase: $\Delta E = E - E_{dehydrated} - N \cdot E_{water}$, where E is the total energy and N is the number of water molecules in the unit cell.

In the next step the optimized structural models were employed for the GIPAW calculation of ^{31}P and ^{27}Al chemical shifts and ^{27}Al quadrupolar coupling constants. The chemical shifts and the quadrupolar parameters were extracted also from the ^{31}P and ^{27}Al MAS NMR spectra. Even though the experimental values obtained at finite temperatures of up to 220 °C are compared to the results of calculations that assume the temperature of 0 K, the agreement between the measured and the calculated ^{31}P and ^{27}Al chemical shifts is reasonably good (Figure 9). This suggests that both experimental techniques, NMR, from which the experimental chemical shifts were obtained, and XRD, which provided structural models for the calculation of chemical shifts, detect equal or very similar structures of the different phases of $AlPO_4$-34. Worse than the agreement in chemical shifts is the agreement in the calculated and experimentally detected ^{27}Al quadrupolar coupling constants. It seems that, as has already been observed with some other materials,[23,24] the degree of hydration and the mobility of water molecules can drastically influence the quadrupolar interaction; the ^{27}Al quadrupolar coupling constants are certainly not a convenient measure for judging the quality of structural models of hydrated porous aluminophosphates.

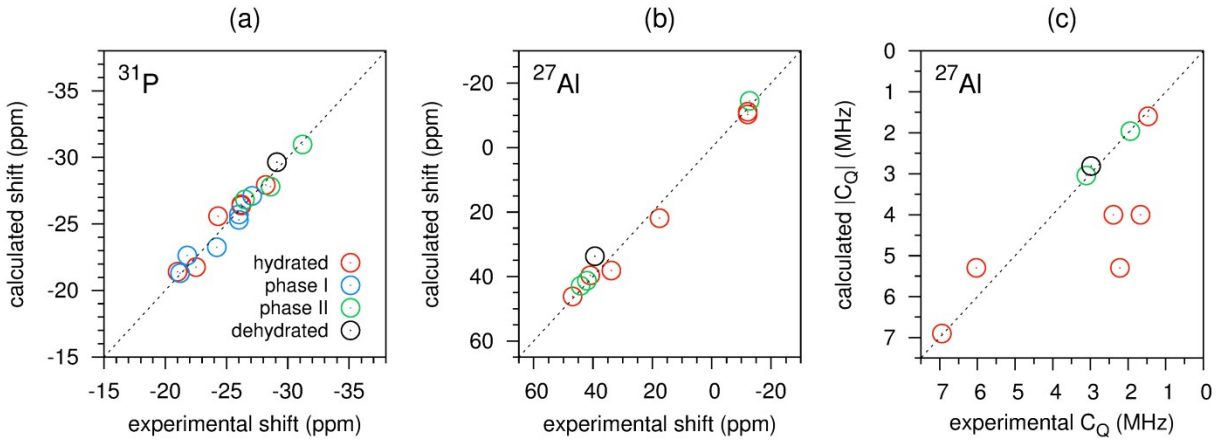

Figure 9. Comparison of the measured and the calculated values of ^{31}P (a) and ^{27}Al (b) isotropic chemical shifts and ^{27}Al quadrupolar coupling constants (c). From the ^{27}Al MAS NMR spectra chemical shifts and quadrupolar coupling constants for the partly dehydrated phase I could not be reliably determined, because the signals belonging to this phase were overlapped with the signals of the partly dehydrated phase II.

Thus, despite the major differences in sample packing, two complementary experimental techniques, NMR and XRD, seem to detect very similar intermediate states during the dehydration of $AlPO_4$-34. Perhaps these intermediate states should not be considered as the states of thermal equilibrium, but rather as selected 'snapshots' during the transition from the fully hydrated phase to the completely dehydrated phase. At least NMR measurements with very small temperature steps (not shown) suggest that the variation of isotropic chemical shifts is quite smooth and continuous. Two snapshots (of phase I and phase II) already allow us to build a more detailed picture of dehydration. Among the 12 water molecules that occupy the unit cell of the fully hydrated form, one located in the double six-ring is very loosely bound and is the first to leave the structure. When being expelled from the structure, this molecule most probably migrates through the small double six-rings and not through the large chabazite cages, which are blocked by a net of strongly hydrogen-bonded water molecules. In each chabazite cage there are eleven water molecules, six of them forming a cluster which interacts with the four water molecules attached to the two six-coordinated Al. The eleventh water molecule is initially attached to the five-coordinated Al site, but detaches from it at only slightly elevated temperatures. Evidently, six-coordinated Al sites are substantially more stable than the five-coordinated sites. Further increase in temperature increases the mobility of water molecules and allows the aluminophosphate framework to adopt higher symmetry. At this higher symmetry it seems to be energetically favourable for the water cluster in the cage to be composed of six rather than of seven molecules, thus one molecule is expelled from the pore. At even higher temperature the coordination bonds between the aluminium atoms and water

molecules break, the hydrogen-bonding network destabilizes, and water very rapidly exits the pores. Although some of these steps have already been predicted by the first-principles calculations, it is this work that provides experimental confirmation for them.

Conclusions

NMR spectroscopy and X-ray diffraction, coupled with first-principles calculations, provided a very detailed insight into the dehydration of $AlPO_4$-34. They showed that this is a very complex process, whose details depend on many parameters. The two experimental techniques were complementary to one another, not only in the sense that XRD yielded information on the average periodic long-range structure and that NMR offered an insight into the local environment of atomic nuclei and on the dynamics within the material, they also worked with very differently packed samples and because of that detected very different dynamics of dehydration. And whereas sensitivity to sample packing may had complicated the comparison of the experimental results obtained by NMR and XRD, the manifestation of this sensitivity also pointed out the very important role that packing of material will have in the potential large-scale applications of $AlPO_4$-34 for energy conversion or heat storage.

Electronic Supplementary Information (ESI) available: Decomposition of the ^{31}P and ^{27}Al MAS NMR spectra of the fully hydrated phase, Rietveld plots, detailed refinement parameters and fractional atomic coordinates for phases I and II.

Acknowledgements

This work was supported by the Slovenian Research Agency (grants P1-0021 and J1-5447). Facilities for the variable-temperature NMR probe development were provided by NMR Institute, Tartu, Riia 181A, Estonia. We would like to thank Edi Kranjc for his help with variable-temperature XRD measurements.

References

1 J. Jänchen, D. Ackermann, E. Weiler, H. Stach and W. Brösicke, *Thermochim. Acta*, 2005, **434**, 37–41.
2 H. van Heyden, G. Munz, L. Schnabel, F. Schmidt, S. Mintova and T. Bein, *Appl. Therm. Eng.*, 2009, **29**, 1514–1522.

3 E.-P. Ng and S. Mintova, *Microporous Mesoporous Mater.*, 2008, **114**, 1–26.
4 S. K. Henninger, F. P. Schmidt and H.-M. Henning, *Appl. Therm. Eng.*, 2010, **30**, 1692–1702.
5 A. Ristić, N. Z. Logar, S. K. Henninger and V. Kaučič, *Adv. Funct. Mater.*, 2012, **22**, 1952–1957.
6 A. Tuel, S. Caldarelli, A. Meden, L. B. McCusker, C. Baerlocher, A. Ristic, N. Rajic, G. Mali and V. Kaucic, *J. Phys. Chem. B*, 2000, **104**, 5697–5705.
7 J. Wu, H. Zhao, N. Li, Q. Luo, C. He, N. Guan and S. Xiang, *CrystEngComm*, 2012, **14**, 8671–8676.
8 A. Cadiau, J. S. Lee, D. Damasceno Borges, P. Fabry, T. Devic, M. T. Wharmby, C. Martineau, D. Foucher, F. Taulelle, C.-H. Jun, Y. K. Hwang, N. Stock, M. F. De Lange, F. Kapteijn, J. Gascon, G. Maurin, J.-S. Chang and C. Serre, *Adv. Mater.*, 2015, **27**, 4775–4780.
9 G. Poulet, P. Sautet and A. Tuel, *J. Phys. Chem. B*, 2002, **106**, 8599–8608.
10 K. Momma and F. Izumi, *J. Appl. Crystallogr.*, 2011, **44**, 1272–1276.
11 T. Takahashi, H. Kawashima, H. Sugisawa and T. Baba, *Solid State Nucl. Magn. Reson.*, 1999, **15**, 119–123.
12 H. C. Torrey, *Phys. Rev.*, 1956, **104**, 563–565.
13 J. Mitchell, T. C. Chandrasekera and L. F. Gladden, *J. Chem. Phys.*, 2010, **132**, 244705.
14 A. Coelho, *Coelho Software*, Brisbane, Australia, 2007.
15 A. Le Bail, H. Duroy and J. L. Fourquet, *Mater. Res. Bull.*, 1988, **23**, 447–452.
16 P. Giannozzi, S. Baroni, N. Bonini, M. Calandra, R. Car, C. Cavazzoni, D. Ceresoli, G. L. Chiarotti, M. Cococcioni, I. Dabo, A. D. Corso, S. de Gironcoli, S. Fabris, G. Fratesi, R. Gebauer, U. Gerstmann, C. Gougoussis, A. Kokalj, M. Lazzeri, L. Martin-Samos, N. Marzari, F. Mauri, R. Mazzarello, S. Paolini, A. Pasquarello, L. Paulatto, C. Sbraccia, S. Scandolo, G. Sclauzero, A. P. Seitsonen, A. Smogunov, P. Umari and R. M. Wentzcovitch, *J. Phys. Condens. Matter*, 2009, **21**, 395502.
17 J. P. Perdew, A. Ruzsinszky, G. I. Csonka, O. A. Vydrov, G. E. Scuseria, L. A. Constantin, X. Zhou and K. Burke, *Phys. Rev. Lett.*, 2008, **100**, 136406.
18 *http://www.qe-forge.org/gf/project/pslibrary*, .
19 C. Pickard and F. Mauri, *Phys. Rev. B*, 2001, **63**.
20 *http://qe-forge.org/gf/project/qe-gipaw/*, .
21 H. J. Monkhorst and J. D. Pack, *Phys. Rev. B*, 1976, **13**, 5188–5192.
22 G. Miceli, S. de Gironcoli and A. Pasquarello, *J. Chem. Phys.*, 2015, **142**, 034501.
23 E. Alvarez, N. Guillou, C. Martineau, B. Bueken, B. Van de Voorde, C. Le Guillouzer, P. Fabry, F. Nouar, F. Taulelle, D. de Vos, J.-S. Chang, K. H. Cho, N. Ramsahye, T. Devic, M. Daturi, G. Maurin and C. Serre, *Angew. Chem. Int. Ed.*, 2015, **54**, 3664–3668.
24 G. Mali, J. Trebosc, C. Martineau and M. Mazaj, *J. Phys. Chem. C*, 2015, **119**, 7831–7841.

Dehydration of $AlPO_4$-34 studied by variable-temperature NMR, XRD and first-principles calculations

Jure Varlec, Andraž Krajnc, Matjaž Mazaj, Alenka Ristić, Kalju Vanatalu, Andres Oss, Ago Samoson, Venčeslav Kaučič and Gregor Mali*

TOC entry

Complementary techniques elucidate water-framework interactions in different states of dehydration, two of which have not been observed before.